EPJ Web of Conferences **86**, 00048 (2015)
DOI: 10.1051/epjconf/ 20158600048

Heavy ion collision dynamics of ^{10,11}B+^{10,11}B reactions

BirBikram Singh[1,a], Manpreet Kaur[1], Varinderjit Kaur[2], and Raj K. Gupta[3]

[1] *Department of physics, Sri Guru Granth Sahib World University, Fatehgarh Sahib-140406, India*
[2] *Mata Gujri College, Fatehgarh Sahib- 140406, India*
[3] *Department of Physics, Panjab University, Chandigarh-160014, India*

Abstract. The dynamical cluster-decay model (DCM) of Gupta and collaborators has been applied successfully to the decay of very-light ($A \sim 30$), light ($A \sim 40-80$), medium, heavy and super-heavy mass compound nuclei for their decay to light particles (evaporation residues, ER), fusion-fission (ff), and quasi-fission (qf) depending on the reaction conditions. We intend to extend here the application of DCM to study the extreme case of decay of very-light nuclear systems ^{20,21,22}Ne* formed in ^{10,11}B+^{10,11}B reactions, for which experimental data is available for their binary symmetric decay (BSD) cross sections, i.e., σ_{BSD}. For the systems under study, the calculations are presented for the σ_{BSD} in terms of their preformation and barrier penetration probabilities P_0 and P. Interesting results are that in the decay of such lighter systems there is a competing reaction mechanism (specifically, the deep inelastic orbiting of non-compound nucleus (nCN) origin) together with ff. We have emipirically estimated the contribution of σ_{nCN}. Moreover, the important role of nuclear structure characteristics via P_0 as well as angular momentum ℓ in the reaction dynamics are explored in the study.

1 Introduction

Compound Nucleus (CN) formed in low energy ($E < 10$ MeV/nucleon) heavy-ion reaction is highly excited and carry large angular momentum ℓ depending upon the energy in the entrance channel and loose it during decay by emitting γ-rays, multiple light particles (LPs: A≤4, Z≤2) like n, p, α or their heavier counterparts (referred to as evaporation residues ER), and fusion-fission (ff) consisting of symmetric and near-symmetric fission fragments, including also the intermediate mass fragments(IMFs)/ clusters [1–5]. In addition to CN decay, non-compound nucleus (nCN) decay may also take place, like the quasi-fission (qf), deep-inelastic (DI) orbitting, etc., and contribute to the overall decay cross section. Reaction dynamics of light mass CN $A \sim 40-80$ has been kind of established as the ff mechanism [4, 5]. In extreme case of very-light compound systems $A \sim 30$, standard rotating liquid drop model (RLDM) predicts strong inhibition of ff as compared to DI scattering process/ orbiting [6]. DI orbiting is referred to as the long lived dinuclear molecular process with strong memory of entrance channel. It is highly motivating to investigate the decay of very-light mass systems for competing reaction mechanims involved in the reaction dynamics. These effects could be small or large enough to compete with ff of CN.

Very light compound systems ^{20,21,22}Ne* formed in ^{10,11}B+^{10,11}B reactions are studied here, for the first time using the Dynamical Cluster-decay Model (DCM) of Gupta and collaborators [4, 5]. The lightest compound system studied so far on the DCM is ^{28}Al* and the results are in good comparison with the available experimental data [5]. It is relevant to mention here that the DCM has been developed to study the decay of hot and rotating CN formed in low-energy heavy ion reaction. It is a non-statistical description of the decay of CN as well as nCN and also to find out the role of rotational energy in the decay of CN. The DCM is so far successfully applied to the decay of a number of compound nuclei in different mass regions [4, 5]. In DCM, the decay of an excited CN is studied as a collective clusterization process for emissions of the LPs, as well as the IMFs and ff, in contrast to the statistical models in which each type of emission is treated on different footing.

The binary symmetric decay (BSD) of very-light mass compound systems ^{20,21,22}Ne* formed in ^{10,11}B+^{10,11}B reactions at $E_{lab} = 48$ MeV and different excitation energies E^*_{CN}, is studied here by using the DCM. The ^{20,21,22}Ne* being negative Q_{out}-value systems would decay only if they are produced in heavy ion reactions with compound nucleus excitation energy sufficiently enough so that

$$E^*_{CN} + Q_{out}(T) = TKE(T) + TXE(T) \qquad (1)$$

where $E^*_{CN} = E_{c.m.} + Q_{in}$, and TXE(T), TKE(T) are total excitation energy and total kinetic energy of the outgoing fragments, respectively (Fig.1(a), (b) and (c)). Within the DCM, the decay of these *lighter* composite systems with comparable size as well as angular momentum, with different excitation energies, is highly interesting to study, keeping in view the expected significant role of nuclear structure (via P_0 here) when a single nucleon is added.

[a] e-mail: birbikram.singh@gmail.com

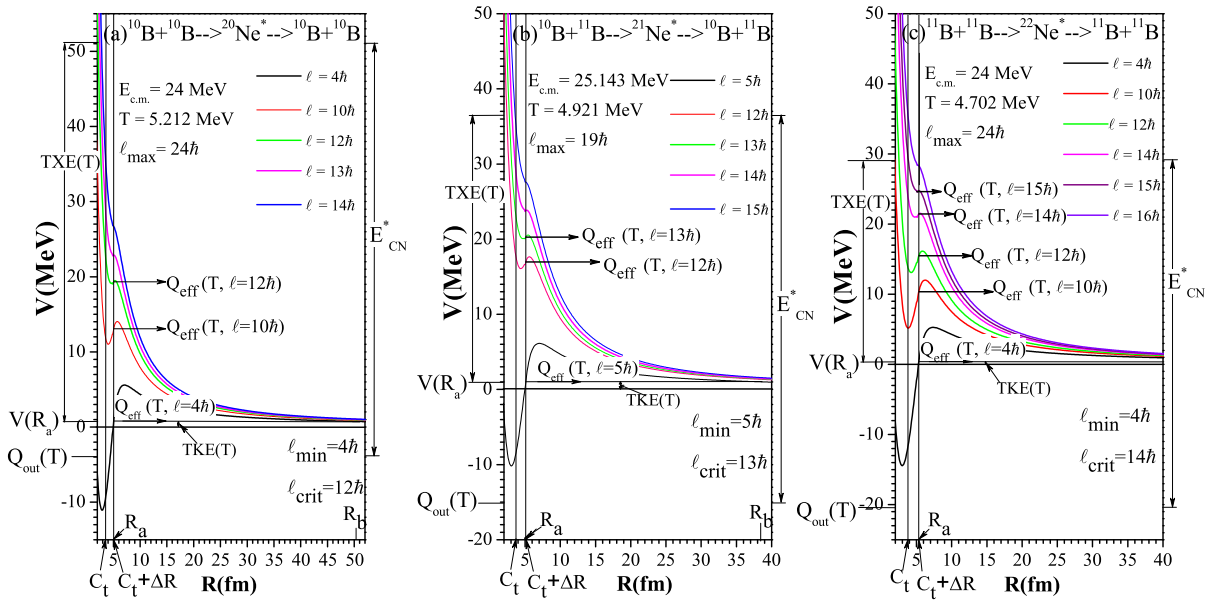

Figure 1. Scattering Potential for the symmetric decay of a) ^{20}Ne*, b) ^{21}Ne*, and c) ^{22}Ne*, at different ℓ-values.

The measured cross sections for the fission like or BSD for the channels ^{10}B+^{10}B, ^{10}B+^{11}B and ^{11}B+^{11}B in the decay of composite systems ^{20}Ne*, ^{21}Ne* and ^{22}Ne* are given, respectively, in an experimental study [7], namely, the measured decay cross section for the binary symmetric decay (BSD) is maximum for ^{20}Ne* ($\sigma_{BSD} \sim 270$ mb) followed by ^{21}Ne* and ^{22}Ne* with their upper limits <130 mb amd <70 mb, respectively. The contribution of σ_{ff} and decay cross sections due to DI orbitting σ_{orb} in the BSD adds to give σ_{BSD}, i.e., $\sigma^{Cal.}_{BSD} = \sigma^{Cal.}_{ff} + \sigma^{Cal.}_{orb}$. Note that all these components are individually measurable quantities. In case, the nCN component σ_{orb} were not measured, it can be estimated empirically from the calculated and measured quantities, as

$$\sigma_{orb} = \sigma^{Expt.}_{BSD} - \sigma^{Cal.}_{ff}. \quad (2)$$

In this work, within the DCM, we attempt to understand the decay behaviour of ^{20,21,22}Ne* and the role nuclear structure as well as angular momentum play in the reaction dynamics of such systems.

A brief description of the DCM is given in Sect. 2. Our calculations, using DCM, are given in Sect. 3. A summary and conclusions of our study are presented in Sect. 4.

2 The Dynamical Cluster-decay Model (DCM)

The DCM [4, 5], based on the quantum mechanical fragmentation theory (QMFT), is worked out in terms of the collective coordinates of mass asymmetry $\eta = \frac{A_1-A_2}{A_1+A_2}$ and relative separation R, which allows to define the decay cross-section, as

$$\sigma = \frac{\pi}{k^2} \sum_{\ell=0}^{\ell_{max/crit}} (2\ell+1) P_0 P; \qquad k = \sqrt{\frac{2\mu E_{c.m.}}{\hbar^2}} \quad (3)$$

in terms of ℓ partial waves, where the preformation probability P_0 refers to η motion and the penetrability P to R motion. With $\mu = mA_1A_2/(A_1 + A_2)$ the reduced mass and ℓ_{max}, the maximum angular momentum, is defined for LPs cross-section $\sigma_{LPs} \to 0$. The ℓ_{crit}-value is the critical ℓ-value, in terms of the bombarding energy $E_{c.m.}$, the reduced mass μ and the first turning point R_a of the entrance channel η_{in}, given by

$$\ell_{crit} = R_a \sqrt{2\mu[E_{c.m.} - V(R_a, \eta_{in}, \ell = 0)]}/\hbar. \quad (4)$$

The tunneling/ penetration probability P is calculated as the WKB integral,

$$P = exp(-\frac{2}{\hbar}\int_{R_a}^{R_b} \{2\mu[V(R,T) - Q_{eff}]\}^{1/2} dR), \quad (5)$$

with first and second turning points, R_a and R_b, (Fig.1(a), (b) and (c)). Note that in Fig.1(c), the value of R_b is not marked since its value is too large (R_b=108.052 fm) to be shown conveniently on the given scale. The choice of parameter R_a in Eq. (5), for a best fit to the data, allows us to relate in a simple way the $V(R_a, \ell)$ to the top of the barrier $V_B(\ell)$ for each ℓ.

In Eq. (3), P_0, the preformation probability referring to η motion, contains the structure information of the compound nucleus, and is the solution of the stationary Schrödinger equation in η, at a fixed R=R_a,

$$\{-\frac{\hbar^2}{2\sqrt{B_{\eta\eta}}}\frac{\partial}{\partial\eta}\frac{1}{\sqrt{B_{\eta\eta}}}\frac{\partial}{\partial\eta} + V(R,\eta,T)\}\psi^\nu(\eta) = E^\nu\psi^\nu(\eta), \quad (6)$$

with

$$P_0(A_i) = |\psi(\eta(A_i))|^2 \sqrt{B_{\eta\eta}}\frac{2}{A}, \quad (7)$$

Here, the mass fragmentation potential $V(\eta, T)$, at fixed $R = R_a$, is the sum of liquid drop energy V_{LDM}, shell

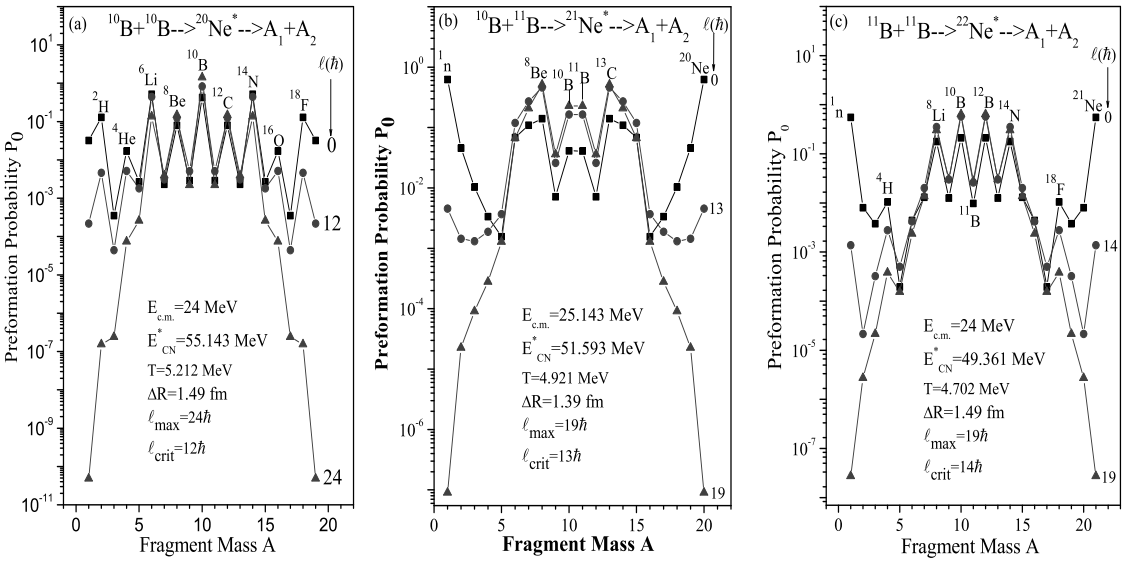

Figure 2. Preformation Probability P_0 as a function of fragment mass A for the decay of a) ^{20}Ne*, b) ^{21}Ne*, and c) ^{22}Ne*, at different ℓ-values.

corrections, Coulomb, nuclear proximity and angular momentum dependent potentials E_C, V_P, V_ℓ, all T-dependent. The mass parameters $B_{\eta\eta}$, defining the kinetic energy term in Hamiltonian, are the smooth classical hydrodynamical masses.

The same equation (3) is used for σ_{nCN} or σ_{orb}, calculated as the DI orbiting (orb) process, since incoming nuclei keep their identity, and hence P_0=1, and then P is calculated for *incoming channel*.

3 Calculations and results

In this section, we present our calculations for the estimation of non-compound nucleus component σ_{nCN} or σ_{orb} (as DI orbitting process) in the BSD of ^{20}Ne*, ^{21}Ne*, and ^{22}Ne* using the DCM. First, we calulate the contribution of σ_{ff} in the BSD and then estimated empirically from the measured and calulated quantities σ_{orb} (= $\sigma^{Expt.}_{BSD} - \sigma^{DCM}_{ff}$).

Fig. 2 shows the variation of P_0 as a function of fragment mass A for the decay of a) ^{20}Ne*, b) ^{21}Ne*, and c) ^{22}Ne*, at different ℓ-values. Fig. 2(a) clearly shows the BSD of ^{20}Ne* formed in ^{10}B+^{10}B at $E_{c.m.} = 24MeV$. Here we note that ^{10}B is strongly favoured at all ℓ-values. On the other hand, BSD of ^{21}Ne* and ^{22}Ne* formed in ^{11}B+^{10}B at $E_{c.m.} = 25.143MeV$ and ^{11}B+^{11}B at $E_{c.m.} = 24MeV$, respectively, are not strongly favoured. Fig. 2(b) shows that the BSD of ^{21}Ne* has competition from ^{8}Be and ^{13}C. Interestingly, in Fig. 2(c) we see that the BSD of ^{22}Ne* in to ^{11}B is least favoured where ^{10}B and ^{12}B are strongly preformed follwed by ^{8}Li and ^{14}N. This result is quite important keeping into view that the experimental data for the $\sigma^{Expt.}_{BSD}$ [7] is maximum for ^{20}Ne* followed by ^{21}Ne* and ^{22}Ne*, as mentioned in the introduction also. Moreover, it is observed in Fig. 2 that the IMFs in the decay of ^{20}Ne*, ^{21}Ne* and ^{22}Ne* are favoured at all the ℓ-values, contrary

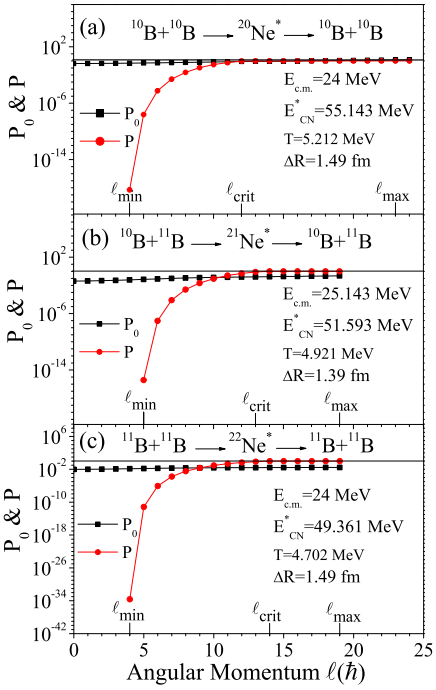

Figure 3. Preformation Probability P_0 and Penetration Probability P as a function ℓ for the symmetric decay of a) ^{20}Ne*, b) ^{21}Ne*, and c) ^{22}Ne*.

to the observation for the decay of very light mass compound nuclei ^{28}Al*, ^{31}P*, ^{32}S* and light mass compound nuclei ^{47}V*, ^{48}Cr*, ^{56}Ni*, where the IMFs are favoured at the higher ℓ-values only [4, 5]. The trend for the LPs observed here is in line with that for the very light as well as light mass compound muclei, i.e., the decay of LPs is favoured at the lower ℓ-values only.

Table 1. The binary symmetric decay cross section calculated using the DCM σ_{ff}^{DCM} for ff process, summed upto $l_{crit}(\hbar)$ for ^{20}Ne*, ^{21}Ne*, and ^{22}Ne*. The experimental data [7] $\sigma_{BSD}^{Expt.}$ is also given here for BSD due to ff as well as the DI orbitting. The contribution of σ_{orb} is estimated from $\sigma_{BSD}^{Expt.} - \sigma_{ff}^{DCM}$.

Compound System	$E_{c.m.}$ (MeV)	E_{CN}^* (MeV)	T (MeV)	l_{max} ($\hbar$)	l_{crit} ($\hbar$)	ΔR (fm)	σ_{ff}^{DCM} (mb)	$\sigma_{BSD}^{Expt.}$ (mb)	σ_{orb} (mb)
^{20}Ne*	24	55.143	5.212	24	12	1.49	195.270	~ 270	74.730
^{21}Ne*	25.143	51.593	4.921	19	13	1.39	65.723	< 130	64.277
^{22}Ne*	24	49.361	4.702	19	14	1.49	8.677	< 70	61.323

In Fig. 1, we notice that the barrier for the BSD of ^{20}Ne*, ^{21}Ne* and ^{22}Ne* starts vanishing at ℓ=12$\hbar$, 13$\hbar$ and 15$\hbar$, respectively. Coincidently, these are ℓ_{crit} values which we obtained from Eq. (4) for these systems. Moreover, value of ℓ_{min} (minimum ℓ value at which WKB integral starts contributing)=4$\hbar$, 5$\hbar$ and 4$\hbar$, respectively for the BSD of ^{20}Ne*, ^{21}Ne* and ^{22}Ne*. We find that the ℓ_{max} values (=24$\hbar$, 19$\hbar$ and 19$\hbar$) for these systems, where $\sigma_{LPs} \rightarrow 0$, are very large in comparison to the ℓ_{crit} values. At these values the scattering potential barrier already vanishes. Therefore, in the present study we have added the contribution of ℓ values upto the ℓ_{crit} values for the respective systems. We also note in Fig. 1 that TXE(MeV) of the outgoing frgaments is maximum for the ^{10}B+^{10}B in the decay of ^{20}Ne*.

Fig. 3(a) shows the variation of P_0 and P as a function ℓ for the symmetric decay of a) ^{20}Ne*, b) ^{21}Ne*, and c) ^{22}Ne*. Comparatively, we find that the P_0 contributes at all the ℓ values whereas P starts contributing at the higher ℓ values only. At ℓ_{crit}, P approaches the maximum value, i.e., near to one. Here we have added the contribution of ℓ values upto the ℓ_{crit} only while calculating the σ_{ff}^{DCM} for the respective systems as given in Table 1. We find that the empirically estimated value of σ_{orb} is maximum for ^{20}Ne* followed by ^{21}Ne* and ^{22}Ne*. Interestingly, we see that the value of ΔR is same for ^{20}Ne* and ^{22}Ne*.

4 Summary and Conclusions

Concluding, the application of DCM is extended to the decay of very light mass compound systems ^{20}Ne*, ^{21}Ne* and ^{22}Ne*. We studied the decay of these systems and calculated σ_{ff} for the BSD as the dynamical fragmentation process. The results clearly point out the dominant BSD for ^{20}Ne* in comparison to other compound systems. P_0 for the IMFs is dominant at all the ℓ-values for all the compound systems. Scattering potentials for the BSD clearly shows the vanishing of the barrier at the respective ℓ_{crit}-values for these systems. The empirically estimated σ_{orb} for the BSD is maximum for ^{20}Ne*. It will be interesting to calculate and observe the contribution of σ_{orb} for nCN decay using Eq. (3) while taking P_0=1 (with P calculated for incoming channels), the relative values of ΔR and their comparison with values fitted for the σ_{ff} in the BSD of the systems studied. Moreover, the present calculations have been done with spherical consideration of the fragments, the effects of the oriented deformed nuclei will be matter of great interest.

Acknowledgement

The authors are thankful to Dr. K. Hagino, Tohoku University (Japan) and Dr. M. Dasgupta, ANU (Australia) for a useful discussion. One of us (B.B.S.) acknowledges the support by the Department of Science and Technology (DST), New Delhi, for this research work, in the form of a Young Scientist Award under the SERC Fast Track Scheme, vide letter No. SR/FTP/PS-013/2011.

References

[1] S. J. Sanders, *Phys. Rev.* C **44**, 2676 (1991); S. J. Sanders, A. Szanto de Toledo and C. Beck, *Phys. Rep.* **311**, 487 (1999).

[2] R. M. Anjos, *et al.*, *Phys. Rev.* C **48**, R2154 (1993); *Phys. Rev.* C **49**, 2018 (1994).

[3] A. Dey, *et al.*, *Phys. Rev.* C **76** 034608 (2007); S. Kundu, *et al.*, *Phys. Rev.* C **78**, 044601 (2008); T. K. Rana, *et al.*, *Phys. Rev.* C **78**, 027602 (2008); M. Ray, *et al.*, *Phys. Rev.* C **78**, 064617 (2008).

[4] Raj K. Gupta *et al.*, *Phys.Rev.* C **68**, 014610 (2003); Lecture Notes in Physics 818, 223, (2010) Ed. C. Beck; *Phys. Rev.* C **88**, 014615 (2013).

[5] B. B. Singh *et al.*, *Int. J. Mod. Phys.* E **15** No. 3, 699 (2006); *Phys. Rev.* C **77**, 054613 (2008); Proc. DAE Symp. on Nuc. Phys. **56**, 474 (2011); **57** 550, (2012); **58**, 380 (2013); Book of Abstracts VI Int. Conf. on Fusion, New Delhi 85, (2014).

[6] P. Möller and J. R. Nix, *Nucl. Phys.* A **361**, 117 (1981); H. J. Krappe, *et al.*, *Phys.Rev.* Lett. **42**, 215 (1979); C. Beck and A. Szanto de Toledo, *Phys. Rev.* C **53**, 1989 (1996).

[7] A. Szanto de Toledo, et al., *Phys. Rev.* Lett. **62**, 1255 (1989).